

Article Info

Received: 02 Apr 2016 | Revised Submission: 20 May 2016 | Accepted: 28 May 2016 | Available Online: 15 Sept 2016

Metallurgical Investigations of Synergic MIG Welding of 304L Stainless Steel

Ravi Butolaa, Mohit Tyagia** and Jitendra Kumarb****

ABSTRACT

The experimental study is carried out for the analysis of weld bead geometry such as bead reinforcement height, bead width and bead penetration of synergic MIG welding of 304L stainless steel. Microstructures of different zones of interest like weld metal, HAZ and fusion boundary under different welding parameters were viewed and captured with an optical microscope coupled with an image analyzing software. Fractured surface of the weld bead specimens were analyzed using Scanning electron microscopy (SEM) to the nature of the fracture mode. The results of EDS analysis shows that the inclusion particle mainly composed of Fe, Cr, Mn, Si, C elements. X ray diffraction (XRD) study has been done and result shows that phases like Fe, Ni-Cr-Fe, and Fe-Cr-Co-Ni are determined.

Keywords: MIG Welding; EDS; XRD.

1.0 Introduction

Synergic MIG is an advanced welding system which incorporates both sprays and pulse transfer. Optimum conditions can be established for a range of applications which are readily reproduced by the welder. Synergic means “to work together” and in connection with the welding process it indicates that the welding machine is capable of choosing the current curve when the welder has set the wire speed, the metal alloy, the wire diameter and the shielding gas.

That is the welding equipment controls the base current, the form and number of the current pulsations. Apart from influencing the bead geometry, the input process variables also affect the metallurgical aspects of the metal being joined.

Austenitic stainless steel is widely used materials in the current industrial area including higher and lower temperature applications such as storage tanks, pressure cups, furnace equipments etc. Using ratio of those materials are increasing constantly due to having superior corrosion resistance and mechanical properties [1-3].

Chen et al. [4] : found that when Cu–Si enriched type 304 SS (containing 2– 2.5 wt. % copper and 1–1.5 wt.% silicon) and a conventional type 304

SS was Welded using gas metal arc welding (GMAW), process ductility decreased and Ferrite levels increased in both weldments, as the heat input was increased. Lee et al. [5] have reported in their studies on effects of strain rate and failure behavior of 304L SS SMAW weldments and find that as the strain rate increases, the flow stress increases and the fracture strain decreases. Milad et al. [6] found that yield and tensile strengths of 304 SS increased gradually at the same rate with increasing degree of cold work. Ghosh et.al. [7].

The austenitic 304 stainless steel is hard machined material, because of its high strain, high strain hardening, and low heat conductivity. When stainless steel is used in a product, the microstructure

Butola et al. [8]. This study show the effect on the microstructure obtained in the heat-affected zone (HAZ) and the carbide zone in the weld metal properties of Casted grey cast iron plates are used as base material. The welding was carried out with manual shielded metal arc welding using ENiFe–Cr filler metal. Butola et al. [9] In this study, bead-on - plate welds were carried out on 304L austenitic stainless steel using Synergic MIG process. In this present investigation 304L having 1.2 mm diameter

*Corresponding Author: Department of Mechanical and Production & Industrial Engineering, Delhi Technological University, Delhi (E-mail: ravibutola33855@gmail.com)

**Department of Mechanical and Production & Industrial Engineering, Delhi Technological University, Delhi

***Department of Mechanical Engineering G.B Pant Govt. Engineering College, Delhi, India

was used as an electrode with direct current electrode positive polarity. Argon and CO₂ was employed for shielding purposes. The fusion zone is generally characterized by a few geometrical features namely bead width, bead height and depth of penetration.

2.0 Experimental Procedure

2.1 Sample preparations

This procedure of preparation of a specimen involves the method of preparing the samples cut out from the plates fit for viewing under a metallurgical microscope. The ultimate objective is to produce a flat, scratch free, mirror like surface. The steps involved in our specimen preparation are as follows:

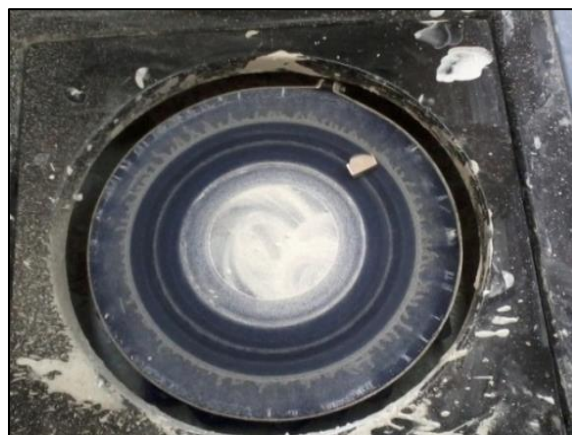
a) Rough grinding: -Our sample is made flat by slowly moving it up and back across the surface of a flat smooth file. Specimen is made rough ground on a belt sander, with the specimen kept cool by frequent dropping in water during grinding operation. The rough grinding is continued until the surface is flat and free of nicks, burrs, etc.

b) Intermediate polishing or grinding: - Grinding is done using rotating discs covered with silicon carbide paper and water. There are a number of grades of paper, with 180,240, 400, 1000, grains of silicon carbide per square inch. 180 grades therefore represent the coarsest particles and this is the grade to begin the grinding operation. Always use light pressure applied at the center of the sample. Continue grinding until all the blemishes have been removed, the sample surface is flat, and all the scratches are in a single orientation. Wash the sample in water and move to the next grade, orienting the scratches from the previous grade normal to the rotation direction. This makes it easy to see when the coarser scratches have all been removed. After the final grinding operation on 1000 paper, the sample is washed in water followed by acetone and dried before moving to the polishers.

c) Fine polishing: - The polishers consist of rotating discs covered with soft cloth impregnated with diamond particles (1 and 0.5 micron size) and an oily lubricant. It began with the 1 micron grade and polishing continued until the grinding scratches have been removed. It is of vital importance that the sample is thoroughly cleaned using soapy water, followed by acetone, and dried before moving onto the final 0.5 micron stage. A properly polished

sample showed only the non-metallic inclusions and will be scratch free.

Fig 1: Polishing Machine.



d) Etching: - The thin layer on the surface which is removed chemically during etching. Secondly, the etchant attacks the surface with preference for those sites with the highest energy, leading to surface relief which allows different crystal orientations, grain boundaries, precipitates, phases and defects to be distinguished in reflected light microscopy. The selection of the appropriate etching reagent is determined by the metal or alloy and the specific structure desired for viewing. In this case I used ferric chloride and hydrochloric acid etching reagent. Its composition is ferric chloride (5g), hydrochloric acid (50ml), and water (10ml). And in this case the etching time is a few seconds to 1 min.

Fig: 2. Samples After Etching



2.2 Using bakelite press

For measurement of micro hardness sample will be flatness. To become flatness we use Automatic mounting press with Bakelite powder. This document provides a step-by-step procedure for mounting a specimen using the Buehler Simplimet 100 automatic specimen mounting press. General familiarity with the objectives and methods of mounting metallographic specimens is assumed. Even so, you should have a experienced person show you how to use this press.

- 1 Apply 2800 psi cold, Plug in heater. Maintain at 2800 psi while heating by pumping as needed. When melted (no further drop in pressure), heat for 1 minutes and then cool for 3 minute by raising heater and using cooling fins.
- 2 Maintain pressure to about 2800 psi, release remaining pressure and press mold out of die.
- 3 Clean die. Thickness of the mount should be sufficient to enable the operator to hold the sample firmly during grinding, but if the mount is too thick, i.e. the powder is too much, it may not be focused very well in the microscope. On the other hand, if too little powder is used; it will cause a lot of problems while using the microscope and especially the hardness tester.

Fig 3: Simplimet 100 Automatic Mounting Press.



Fig 4: Heat time and cool time of Automatic Mounting press.

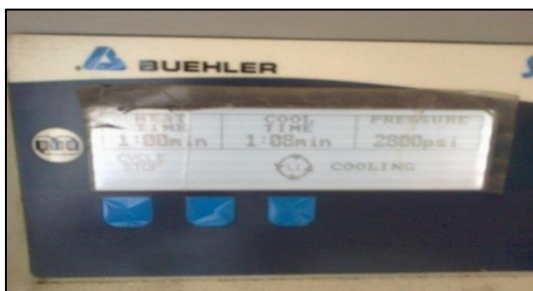


Fig 5: Sample prepares.



The Simplimet 3 is an automatic electro-hydraulic specimen mounting press. To mount a specimen the operator simply loads the press, starts the automatic molding sequence and pre-heating for some time and then heating for 1 minute after complete heating time then cool time start for 3 minute returns 5 to 10 minutes later to remove a cool mounted sample.

The essential specifications of the Simplimet 3 include a maximum 200°C molding temperature which can be specified in 10°C steps, 0 to 4400 psi mounting pressure in 10 psi steps, 1 second to 30 minute molding time and a 100 psi pre-load.

3.0 Results and Discussion

3.1 Micro structural analysis

Microstructure is defined as the structure of a prepared surface or thin foil of material as revealed by a microscope above 25× magnification.

The microstructure of a material can strongly influence physical properties such as strength, toughness, ductility, hardness, corrosion resistance, high/low temperature behavior, wear resistance, and so on, which in turn govern the application of these materials in industrial practice.

The micro structural features of a given material may vary greatly when observed at different length scales. For this reason, it is crucial to consider the length scale of the observations when describing the microstructure of a material.

To study the Microstructure Olympus GX 41 microscope was used in conjunction with META-Lite Software.

Fig 6: Olympus GX 41MICROSCOPE



Fig 7: (a) Sample 2

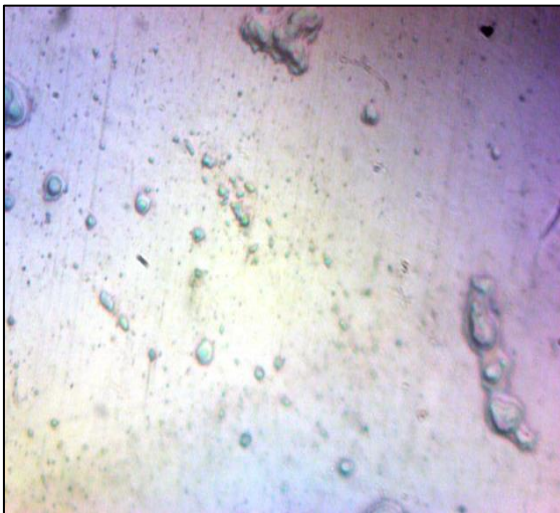


Fig 7: (b) Sample 4

Fig: 7 Micro structures at magnification 100x.90

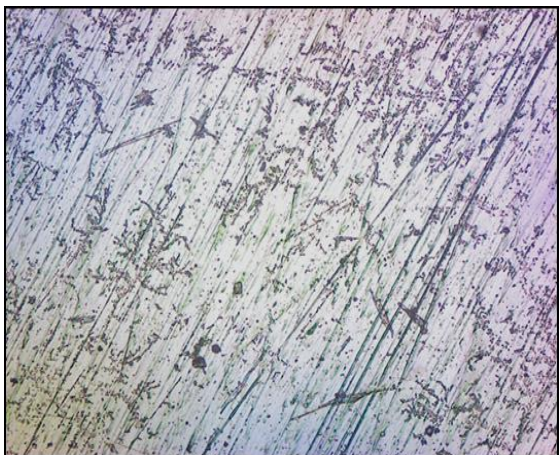


Fig 8 (a): Sample 15

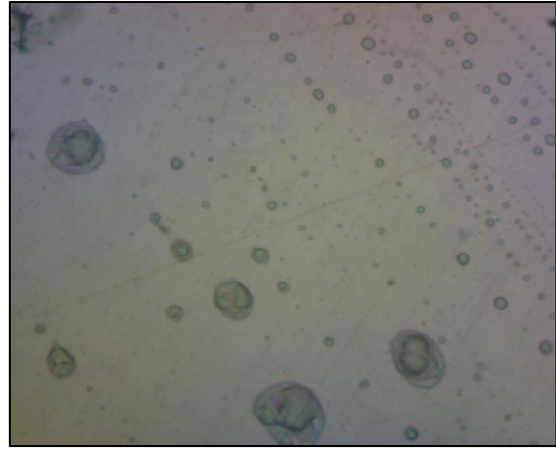


Fig 8: (b) Sample 24

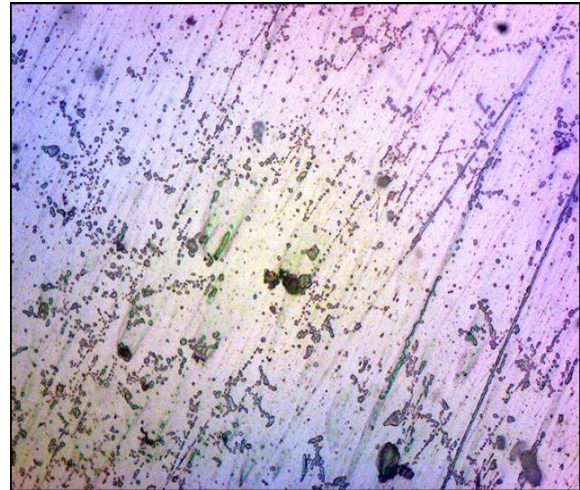


Fig 8: Micro structure at magnification 50x.75 The microstructure is shown above. In the microstructure the inclusions and porosity were found. These inclusions and porosity may be due to atmospheric gas in the shielding gas composition. The size of pores and inclusions are small as current increases base material microstructure is presented. When the temperature is very high water disintegrates into H₂ and O₂ and as H₂ comes out it leaves large no of fine holes on the surface of welded part.

Figure7. (a) Sample 2 Spatter occurs when the weld puddle expels molten metal and scatters it along the weld bead, this molten metal then cools and forms a solid mass on the work piece. Excessive spatter not only creates a poor weld appearance, but it can also lead to incomplete fusion in multiple welding pass applications.

3.2 Energy dispersive spectroscopy (EDS)

Energy Dispersive Spectroscopy (EDS) allows one to identify what those particular elements are and their relative proportions (Atomic % for example). Below is a secondary electron image of a polished

geological specimen and the corresponding X-ray spectra that was generated from the entire scan area. The Y-axis shows the counts (number of X-rays received and processed by the detector) and the X-axis shows the energy level of those counts.

Table: 1 Elemental Compositions of Sample

| <i>Element</i> | <i>Net</i> | <i>Int.</i> | <i>Weight %</i> | <i>Weight %</i> | <i>Atom %</i> | <i>Atom %</i> | <i>Formula</i> | <i>Standard</i> |
|----------------|---------------|---------------|-----------------|-----------------|---------------|---------------|----------------|-----------------|
| <i>Line</i> | <i>Counts</i> | <i>Cps/nA</i> | | <i>Error</i> | | <i>Error</i> | | <i>Name</i> |
| <i>Cr K</i> | 1652 | 0.001 | 19.78 | +/- 0.97 | 21.02 | +/- 1.03 | Cr | |
| <i>Cr L</i> | 1059 | 0.000 | --- | --- | --- | --- | | |
| <i>Fe K</i> | 3563 | 0.001 | 71.95 | +/- 2.42 | 71.19 | +/- 2.40 | Fe | |
| <i>Fe L</i> | 2339 | 0.001 | --- | --- | --- | --- | | |
| <i>Ni K</i> | 252 | 0.000 | 8.27 | +/- 1.12 | 7.78 | +/- 1.05 | Ni | |
| <i>Ni L</i> | 387 | 0.000 | --- | --- | --- | --- | | |
| <i>Total</i> | | | 100.00 | | 100.00 | | | |

Fig 9: EDS Analysis Welded Specimen

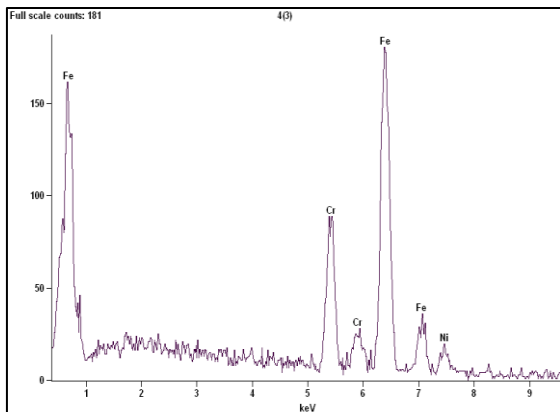


Fig 10: SEM Image of Welded Specimen

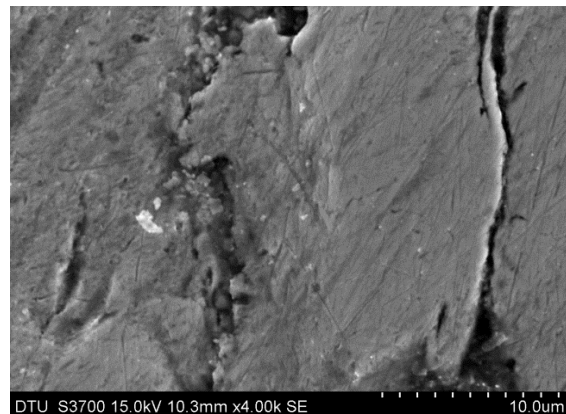
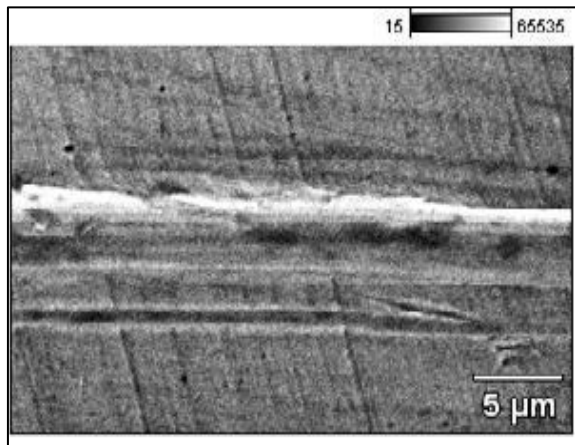
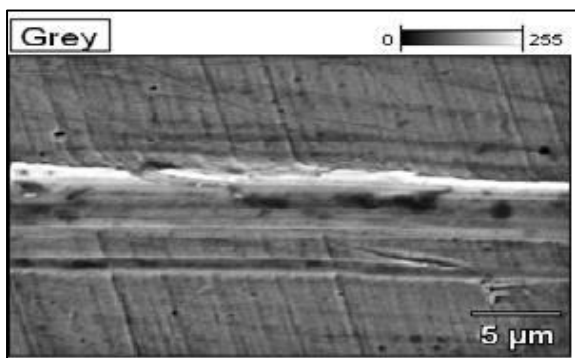


Fig 11: Elemental COMPOSITIONS SAMPLE

**Fig 11: (a) Data Type: Counts Mag: 4000
Acc. Voltage: 15.0 kV**



**Fig 11: (b) Data Type Counts Mag: 4000
Acc. Voltage: 15.0 kV**



**Fig 11: (c) Data Type: Counts Mag: 4000
Acc. Voltage: 15.0 kV**

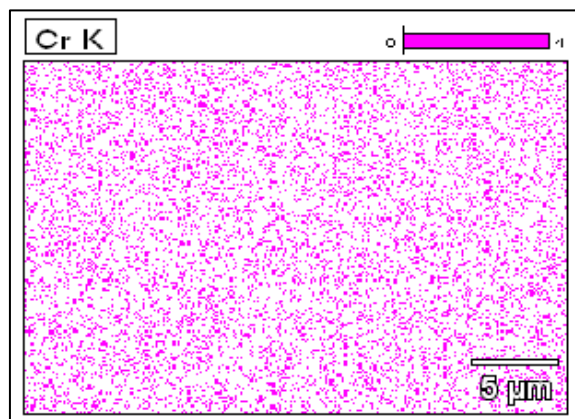


**Fig 11: (d) Data Type: Counts Mag: 4000
Acc. Voltage: 15.0 kV**

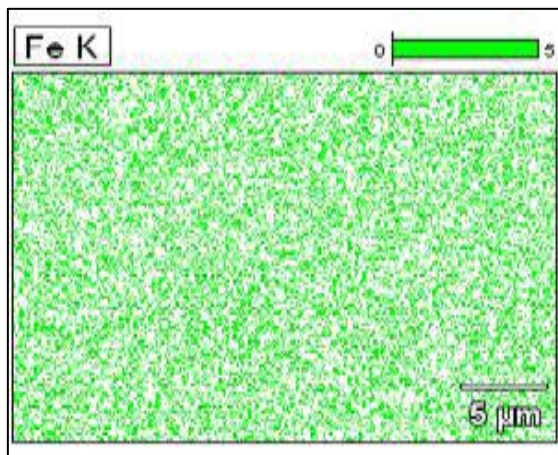
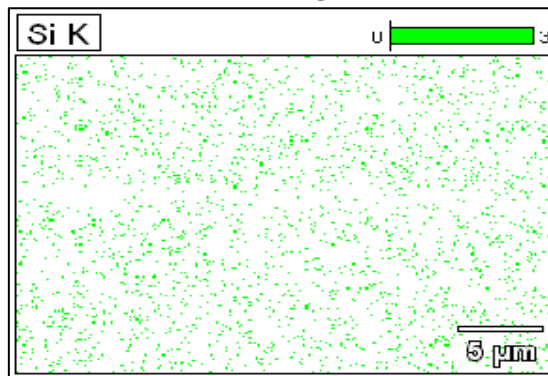
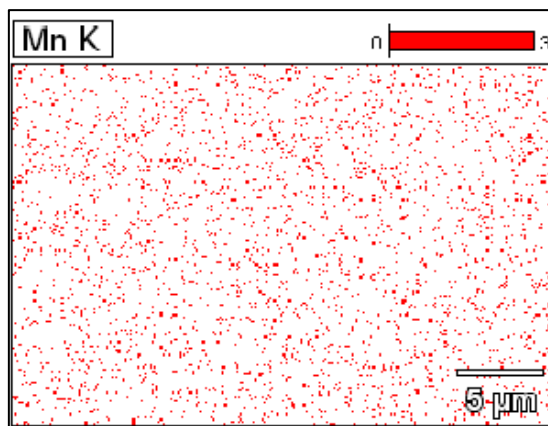


Fig 12: Elemental compositions Sample

**Fig 12: (a) Data Type Counts Mag: 4000
Acc. Voltage: 15.0 kV**



**Fig 12: (b) Data Type: Counts Mag: 4000
Acc. Voltage: 15.0 kV**



**Fig 12: (c) Data Type: Counts Mag: 4000 Acc.
Voltage: 15.0 kV**

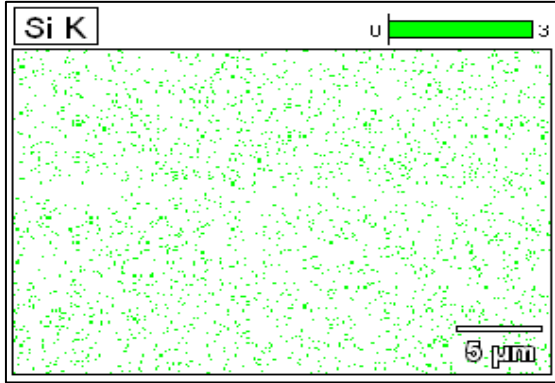
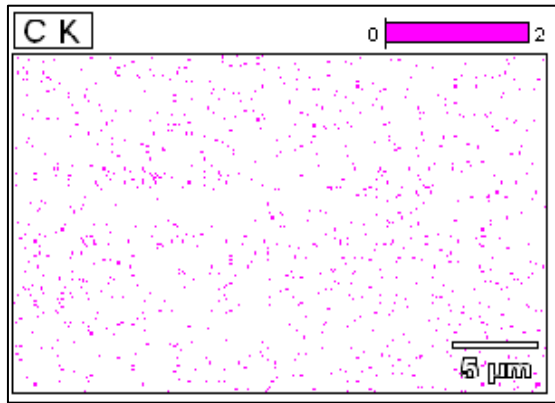


**Fig 12 (d): Data Type Counts Mag: 4000 Acc.
Voltage: 15.0 kV**

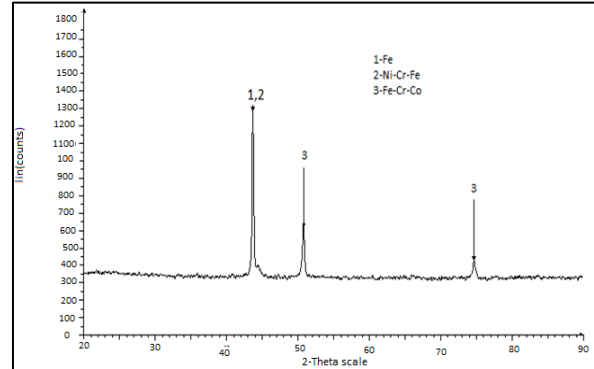


The results of EDS analysis presented in Fig 11 and fig 12 shows that the inclusion particle mainly composed of Fe, Cr, Mn, Si, C elements. During welding, the shielding gas interacts with the weld pool and the addition of CO₂ and or O₂ in argon causes oxidation, which results in some losses of alloy constituents and produces inclusions in the weld.

3.3 X-ray Diffraction Technique (XRD)

The purpose of this study was to investigate the metallurgical phases of 304L SS joints prepared by synergic MIG welding, using the X-ray diffraction technique (XRD), XRD analysis were performed at room temperature. X-ray scattering techniques are a family of non-destructive analytical techniques which reveal information about the crystallographic structure, chemical composition, and physical properties of materials.

**Fig 13: XRD Analysis of Welded Specimen
Sample 2 and Sample 4**



In the XRD analysis, like Fe, Ni-Cr-Fe, and Fe-Cr-Co-Ni phases were determined as shown in above Fig 13 the diffractive peaks of 1, 2, 3 phase could be observed. It was observed that peaks 1, 2 and 3 formed at 43.688°, 50.719° and 74.699° respectively.

4.0 Conclusions

The metallurgical investigation and microscopic study has been done on Olympus GX 41 microscope. It was observed that the spatter has been seen for sample 2 and, pin hole and blow hole has been seen in the sample in above figure. Fractured surface of the weld bead specimens were analysis using Scanning electron microscopy (SEM) to the nature of the fracture mode of the welded sample. In order to identify the phase constituents of the weld metal, X-ray diffraction test is performed on the specimen, cut from the weld metal. In Fig 13. The diffractive peaks of 1, 2, 3 phase could be observed. It was observed that peaks 1, 2 and 3 formed at 43.6460, 50.7580 and 74.7690 respectively.

References

- [1] Odabaş, C. Paslanmaz Çelikler, Temel Özellikleri, Kullanım Alanları, Kaynak Yöntemler, Askaynak-İstanbul, 2002.
- [2] Smith, W.F.: "Paslanmaz Çelikler", Mühendislik Alaşımlarının Yapı ve Özellikleri, Bölüm 5, Cilt 1, Transl.by: Erdoğan, M., Ankara, 2000, 169-214.

- [3] Lin, Y.C.; Chen, P.Y.: "Effect of Preheating on The Residual Stress in Type 304 Stainless Weldment", *Journal of Materials Processing Technology*, 63, 1997, 797-801.
- [4] Chen, T.F., Chen, Y.R., Wu, W. Properties of Cu-Si enriched type 304 stainless steel welds. *Sci. Techno Weld Joining*; 3, 1998, 75-9.
- [5] Lee W.S., T zeng F.T., Lin C.F. "Mechanical properties of 304L stainless steel SMAW joints under dynamic impact loading". *Journal of Material Science*; 40: 483-947.(2005)
- [6] Milad M, Zreiba N, Elhalouani F, Baradai C. The effect of cold work on structure and properties of AISI 304 stainless steel. *J Mater Process Technol*; 203, 2008, 80-5.
- [7] Ghosh. S, Kain.V, Microstructural changes in AISI 304L stainless steel due to surface machining: effect on its susceptibility to chloride stress corrosion cracking, *Journal of Nuclear Materials*, 403, 20106, 2-67.
- [8] Butola. R, Kumar. J, Verma. V, Mahara. P, Study of Microstructure, Impact Strength on Manual Metal Arc Welding Of Gray Cast Iron Using ENiFe-CI Filler Metal, *IOSR Journal of Engineering*, 37-42, July, 2013.
- [9] Butola. R, Meena. S L, Kumar. J, "Effect of Welding Parameter on Micro Hardness of Synergic MIG Welding of 304l Austenitic Stainless Steel", *International Journal of Mechanical Engineering & Technology*, 4(3), 2013, 337 - 343.